

COMPOSABLE SYSTEM SIMULATION OF DISPERSION IN COMPLEX ELECTROPHORETIC SEPARATION MICROCHIPS

Y. Wang, Q. Lin, T. Mukherjee

Carnegie Mellon University, Pittsburgh, PA, USA, yiw@andrew.cmu.edu

ABSTRACT

This paper presents a composable system simulation framework for electrophoretic separation microchips, using an analog hardware description language integrating analytical dispersion models that describe not only the behavior of individual components, but also the interactions between them. Both DC and transient analysis are performed in the framework. The accuracy (relative error less than 10%) and tremendous speedup (100~10,000×) of composable system simulations are verified by comparison to experiment and numerical studies.

Keywords: dispersion, system simulation, electrophoretic separation microchips

1 INTRODUCTION

While electrophoretic separation microchips have been widely studied in the past decade, their efficient simulation and design at the system-level continues to be a challenge. Experimental trial-and-error and numerical computation methods can lead to unacceptably long design cycles. Several analytical [1, 2] and semi-analytical [3] models and simulations of analyte band broadening (dispersion) have been proposed to speed up design at the component-level. A system simulation approach in which a design is decomposed into components has been presented [4], but involves over-simplified dispersion models that do not accurately account for component interactions and still require users with expert knowledge. To address these issues, this paper presents a composable system simulation framework using an analog hardware description language (Verilog-A) integrating analytical dispersion models [5] that are capable of capturing the interactions between components. The simulations illustrate the effect of chip topology, analyte properties and buffer properties on separation performance. Thus, it is generally applicable to the design of practical electrophoretic microchip devices.

2 COMPOSABLE SYSTEM SIMULATION

Our composable simulation framework consists of a model library and simulation engine. One major contribution over [5] is the development of a Verilog-A library consisting of parameterized behavioral models for commonly used components in separation microchips. Users can compose a complex design schematic by wiring

these blocks for a fast and reliable top-down iterative approach to system-level design. Figure 1 illustrates two practical electrophoresis systems (serpentine and spiral) and their schematics. The systems are decomposed into a set of components including reservoirs, detector, injector, straight channels and turns, which are then linked via interface parameters according to the spatial layout and physics. Cadence is used to netlist the structure of the composable network and Spectre is employed as the simulator in this paper as in [6] (other schematic editors and simulators capable of simulating Verilog-A can also be used).

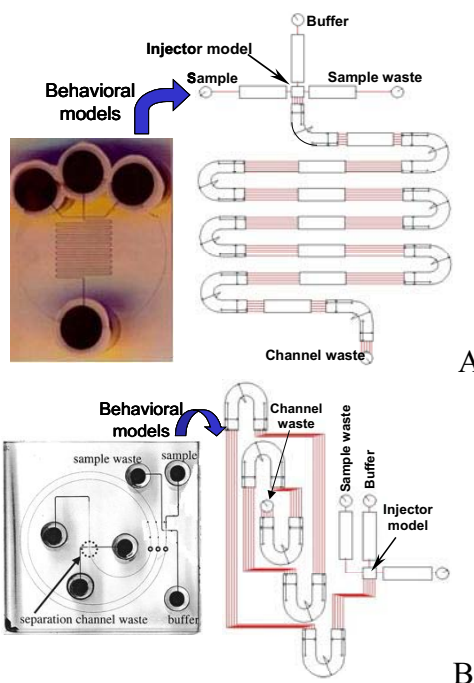


Figure 1: Serpentine (A) and spiral (B) electrophoretic separation microchips (Left) and their schematics (Right) with analog hardware description behavioral models

2.1 Interface parameters

The first step in creating a composable model of a system is to identify the parameters that will be communicated between neighboring components (interface parameters). There are two kinds of interface parameters involved in the network. One is the nodal voltage globally determined by Ohm's and Kirchhoff's laws. The other pertains to dispersion and includes variance (σ^2), the longitudinal standard deviation of the cross-sectional average concentration; skew coefficients (B_m), used to

describe the skew caused by the turns; separation time (t), the moment the center of mass of the band reaches the component; and amplitude (A), the maximum concentration. Since the dispersion occurring in the downstream component doesn't affect the upstream, the parameters related to dispersion are calculated using a directional signal flow in which the output from one component is assigned as the input to the next, starting from an injector.

2.2 Behavioral Models

After selecting the interface parameters, the second step in developing a composable model library is selecting the list of composable elements, and deriving behavioral models for each element. Our composable library consists of seven basic models, which include turns (90° or 180°, clockwise or counter-clockwise), straight channel, injector and detector. The goal of each behavioral model is to capture the input-output signal flow relationship between the dispersion interface parameters and the equivalent Kirchhoffian electric network for the voltage interface parameter (see Figure 2). In a simulation scheme, the steady nodal voltage and the electric field through the component will be determined first. Users only need to input the voltages applied on all reservoirs as boundary conditions, and the simulator is able to calculate the nodal voltage distribution, which is another new feature beyond [4, 5]. Based on the computed electric field (E), the input-output functions of the dispersion interface parameters are then calculated. The inherent variable for the functions is the residence time Δt in a component.

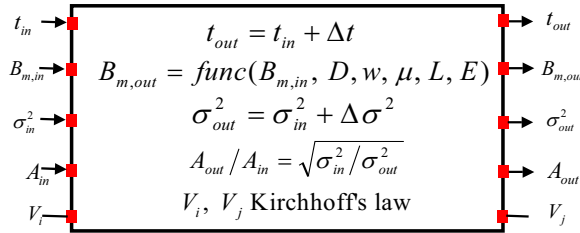


Figure 2: Structure of the behavioral model for composable system simulation. The arrow indicates the direction of signal flow for dispersion computation, and subscripts “in” and “out” represent the input and output to the model.

The residence time and amplitude ratio through a component is given as

$$\Delta t = L/E\mu \quad (1)$$

$$A_{out}/A_{in} = \sqrt{\sigma_{in}^2/\sigma_{out}^2} \quad (2)$$

where μ is the electrophoretic mobility of the species, L is the longitudinal length of the component; for a turn, $L=\theta R_c$ and θ is the angle of the turn. To obtain Eq (2), we always assume a Gaussian concentration distribution for the analyte band in the system.

The change of skew coefficients and variance depends on the specific component [5]. For a straight channel,

$$B_{m,out} = B_{m,in} \cdot e^{-(m\pi)^2 \Delta t D/w^2} \quad (3)$$

$$\Delta\sigma^2 = 2D \cdot \Delta t \quad (4)$$

For a turn,

$$B_{m,out} = \begin{cases} \pm \frac{4\theta(1-(-1)^m)(1-e^{-\lambda_m \Delta t D/w^2})}{(m\pi)^4 \Delta t D/w^2} + B_{m,in} e^{-\lambda_m \Delta t D/w^2} & , m \neq 0 \\ B_{m,in} & , m = 0 \end{cases} \quad (5)$$

$$\Delta\sigma^2 = 2D\Delta t \pm \frac{8w^4\theta}{D\Delta t} \sum_{m=odd} \left(\frac{B_{m,in} (1-e^{-(m\pi)^2 D\Delta t/w^2})}{(m\pi)^4} \right) + \frac{64w^6\theta^2}{(D\Delta t)^2} \sum_{m=odd} \frac{(-1+e^{-(m\pi)^2 D\Delta t/w^2} + (m\pi)^2 D\Delta t/w^2)}{(m\pi)^8} \quad (6)$$

where w is the channel width, D is the molecular diffusivity of the species, $m=0,1,2,3\dots$. In Eq. (5) and (6), the plus sign is assigned to the first turn and any turn increasing the skew caused by the first; the minus sign is assigned to any undoing the skew.

To initiate and detect the dispersion, models of injector and detector are needed. Currently the injector model (see Figure 1) requires the user to specify its skew coefficients (B_m) and variance, which will be replaced with a detailed model from [7] when available.

In the detector model, the skew coefficient is transferred without change due to the small detection length L_{det} . The variance associated with the length is given as [8]

$$\Delta\sigma^2 = L_{det}^2/12 \quad (7)$$

The detector model generates an electropherogram (concentration vs. time) when the system is simulated using transient analysis. Spectre will first calculate DC operating points. Based on these points, the transient simulation is then performed by scanning the read-out time. Assuming the band doesn't substantially spread out during its passing through the detector, we approximate the cross sectional average concentration output (C_m) as

$$C_m = A_{out} \cdot e^{-(E\mu)^2(t-t_{out})^2/2\sigma_{out}^2} \quad (8)$$

where A_{out} , t_{out} and σ_{out}^2 are detector outputs from DC analysis; t is the actual read-out time.

3 RESULTS AND DISCUSSION

Our composable system simulation results are shown in Figures 3-6. In Figure 3A, an electrophoresis column of two complimentary turns used to separate TRITC-Arg is

compared to our DC system simulations, showing excellent agreement. According to [5], the final variance normalized by w^2 depends on two dimensionless times τ_t and τ_s , the ratio of the time for an analyte molecule to advect through a channel to the time for it to diffuse across the channel width ($\tau = \Delta t D / w^2$, τ_t is the dimensionless time in the turn and τ_s in the inter-turn straight channel). In this simulation, $\tau_t = 0.068$ is relatively small, and transverse diffusion in the turn does not have enough time to remove all of the turn-induced skew, which accordingly incurs abrupt increase in variance (see the skewed band after the first turn in the numerical simulation plot in Figure 3A). During an analyte's migration in the long inter-turn straight channel, the transverse diffusion has adequate time (relatively high $\tau_s = 0.696$) to smear out most of the skew and presents a nearly uniform band before the second turn. The second turn then distorts the band again in the opposite direction, leading to another turn-induced variance equal to the one caused by the first turn. Figure 3B shows electropherograms from three detectors placed in the system. Respectively their positions are before the first turn, in the inter-turn straight channel, and after the second turn. Since both turns broaden the analyte band, the amplitude decreases consecutively and the band spreads out, where an initial band with variance $\sigma^2 = 100 \mu\text{m}^2$ and normalized amplitude $A = 1$ was injected.

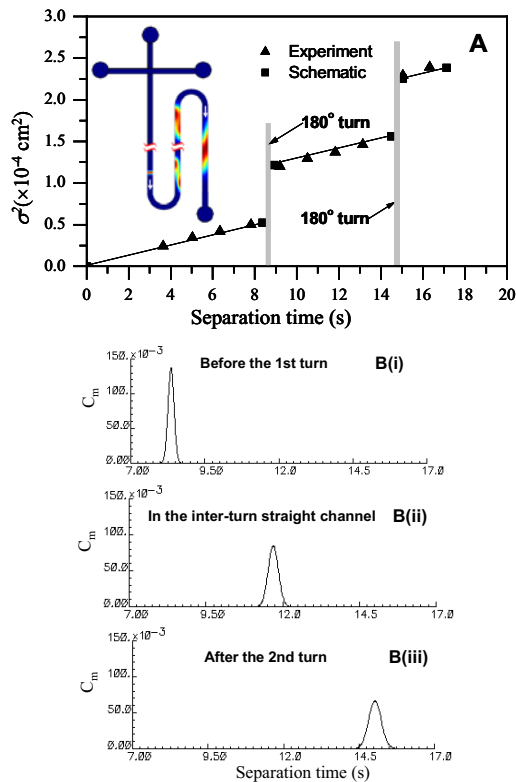


Figure 3: Comparison of experimental data [3] with DC system simulation (A) at $\tau_t = 0.068$ and $\tau_s = 0.696$. The mean width 50 mm [1] and diffusivity $3.12 \times 10^{-10} \text{ m}^2/\text{s}$ were used in the simulation. Transient analysis (B) simulates three detectors' read-outs.

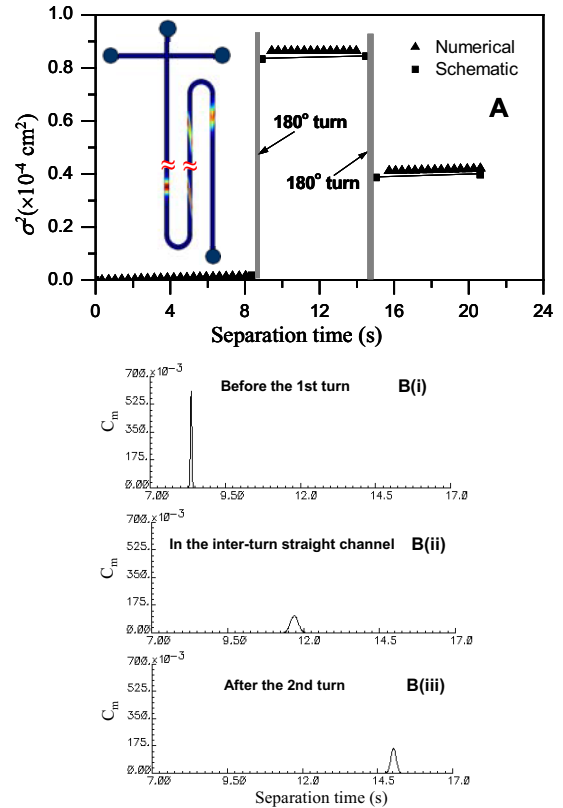


Figure 4: Comparison of DC system (A) simulation to numerical results at $\tau_t = 2.2 \times 10^{-3}$ and $\tau_s = 2.23 \times 10^{-2}$. Diffusivity of $1 \times 10^{-11} \text{ m}^2/\text{s}$ was used in the simulation. Transient analysis (B) simulates three detectors' read-out.

In Figure 4, numerical and composable simulations are conducted, in which all parameters in Figure 3 are kept unchanged except for a very low diffusivity (common for DNA sequencing in gels or matrix materials), rendering extremely low $\tau_t = 2.2 \times 10^{-3}$ and $\tau_s = 2.23 \times 10^{-2}$. A maximum relative error of 5.6% is found. Netlisting and DC simulation take 50 seconds for the first time, and less than a second for subsequent iterations, leading to a $150 \sim 7,500 \times$ speedup. In this example, the longitudinal molecular diffusion is very small, inferred by the nearly zero change of variance in the straight channel; and the convection is significant in the total dispersion. Hence the analyte band keeps its sharp skew before arriving at the second turn that corrects most of the skew and leads to a reduced final variance. This indicates the importance of individual system level simulation and design for different species analysis. The transient simulation shows different concentration read-outs of the three detectors, compared to Figure 3B. Due to less dispersion of the analyte band, all detectors in Figure 4B show better performance compared to Figure 3B, as seen by the higher concentration output in Figure 4B. Because of the skew correction and dispersion reduction by the 2nd turn, the detector after the second turn shows a higher peak and narrower band than that in the inter-turn straight channel. This shows that for the microchip electrophoresis of low-diffusivity species, e.g.

the DNA in gels or other matrix materials that further reduce the diffusion coefficient, even numbers of turns should be applied to take advantage of the skew canceling interactions caused by complimentary turn pairs.

In Figure 5, a serpentine electrophoretic separation system (similar to Figure 1) involving six complimentary turns is simulated and compared to numerical results. The variance growth at the outlets of the second, the fourth and the sixth turn are extracted. A worst-case error of 9.5% at the lowest τ_t and τ_s , and a 600~15,000 \times speedup are obtained. An observation can be made here that the variance increases with the even number of complimentary turns in a superlinear to sublinear manner depending on τ_t and τ_s [9].

In Figure 6, a complex spiral separation microchip of five turns to separate Dichlorofluorescein is simulated and compared to experimental results. A worst-case error of 12% on plate number is found. The linear growth of plate number with electric field confirms that molecular diffusion is the major dispersion source in such a system [10].

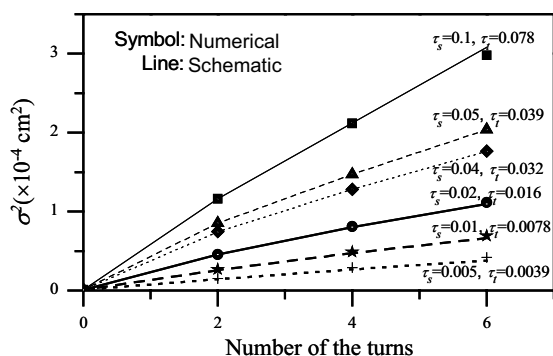


Figure 5: Comparison of composable serpentine system simulation (lines) to numerical results (symbols). τ_t and τ_s range from 0.078 to 0.0039 and from 0.1 to 0.005 respectively. The detections of the analyte band's variance are taken at the outlets of the second, the fourth and the sixth turns.

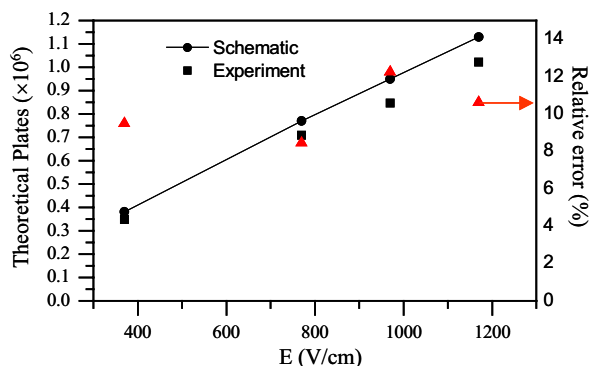


Figure 6: Comparison of composable spiral system simulation to experimental data on theoretical plate number vs. electric field. Right axis shows the relative error between simulation and experiments

4 CONCLUSION

A composable system simulation framework for complex electrophoretic separation microchips has been presented, in which a parameterized behavioral model library using an analog hardware description language (Verilog-A) has been developed. Kirchhoff's law and directional signal flow have been employed to solve the electric and dispersion network respectively. The system simulation results have been verified by numerical and experimental data. The proposed interface parameters and behavioral models are able to accurately capture the combined effects of system topology and parameters (such as analyte and buffer properties) on the separation performance. The transient analysis is also conducted to intuitively observe the actual detector read-out of the cross-sectional average concentration. Compared to numerical methods, a tremendous speedup (100~10,000 \times) can be achieved by the composable simulation, while still maintaining high accuracy (relative error less than 10%). This enables the sub-hour system-level synthesis and optimal design of electrophoretic separation microchips [11].

ACKNOWLEDGEMENT

This research is sponsored by the DARPA and the Air Force Research Laboratory, Air Force Material Command, USAF, under grant number F30602-01-2-0587, and the NSF ITR program under award number CCR-0325344.

REFERENCES

- [1] S.K. Griffiths and R.H. Nilson, *Anal. Chem.*, 72, 5473, 2000.
- [2] J.I. Molho *et al.*, *Anal. Chem.*, 73, 1350, 2001.
- [3] C.T. Culbertson, S.C. Jacobson and J.M. Ramsey, *Anal. Chem.*, 70, 3781, 1998.
- [4] Coventor Inc. "Behavioral Models for Microfluidics Simulations," CoventorWare, 2001.
- [5] Y. Wang, Q. Lin, T. Mukherjee, *MicroTAS'03*, 135, 2003.
- [6] Q. Jing, T. Mukherjee and G.K. Fedder. *ICCAD'02*, 10, 2002.
- [7] R. Magargle, J.F. Hoburg, T. Mukherjee. *NanoTech 2004*, (accepted), 2004
- [8] S.C. Jacobson, C.T. Culbertson, J.E. Daler and J.M. Ramsey. *Anal. Chem.* 70, 3476, 1998.
- [9] R.M. Magargle, J.F. Hoburg and T. Mukherjee. *MSM'03*, 214, 2003.
- [10] C.T. Culbertson, S.C. Jacobson and J.M. Ramsey. *Anal. Chem.*, 72, 5814, 2000.
- [11] A.J. Pfeiffer, T. Mukherjee, S. Huan. *IMECE'03*, 2003.